Nanoscale

COMMUNICATION

Check for updates

Dual-signalled magneto-optical barcodes with lanthanide-based molecular cluster-aggregates†

Diogo Alves Gálico and Muralee Murugesu (iD) *

A proof-of-concept for magneto-optical barcodes is demonstrated for the first time. The dual-signalled spectrum observed *via* magnetic circular dichroism spectroscopy can be used to develop anti-counterfeiting materials with extra layers of security when compared with the widely studied luminescent barcodes.

Counterfeit merchandise and forged documents pose significant challenges for governments, companies, and consumers, leading to substantial financial losses and potential health and environmental hazards.[1–3] The severe consequences of counterfeit items demand rapid advancements in anti-counterfeiting technologies, aiming to stay one step ahead of forgers. Monochrome barcodes and hologram anti-counterfeit technologies have been widely used to uniquely identify and secure products, but the basic characteristics of these security labels make them vulnerable to duplication.[4,5]

Considering these issues, researchers have introduced lanthanide-based luminescent materials with one or more emitter centres, creating intricate optical barcodes.[6–13] The intrinsic narrow emission bands characteristic of each lanthanide ion and the presence of a unique spectral fingerprint, depending on the crystal-field surrounding the lanthanide ion,[14,15] make them an attractive choice when aiming for more secure optical barcodes. For these luminescent barcodes, the read-out can be realized by the naked eye or by using an emission detector.

Despite all the efforts and remarkable progress, it is still possible to replicate luminescent barcodes by mixing different emitters in an appropriate ratio to simulate the same colour output or similar ratio between the emission bands. The use of relatively high-resolution spectrometers is also preferred in order to properly differentiate the emission fingerprint

Department of Chemistry and Biomolecular Sciences, University of Ottawa,
10 Marie Curie, Ottawa, Ontario, K1N 6N5, Canada.
E-mail: m.murugesu@uottawa.ca

between different luminescent barcodes, which limits the use of handheld or portable detection systems.

Hence, incorporating a dual-signalled spectral signature would introduce an extra layer of protection. Polarized absorption/emission techniques, such as circular dichroism (CD) and circularly polarized luminescence (CPL), could be used to attain these features.[16–18] Implementing positive and negative bands in a CD and CPL security approach could elevate the security level of optical barcodes.[16]

With that said, exploring magnetically induced polarization could take security features to a whole new level. By switching the direction of the applied magnetic field, the dual-signalled spectral signature can be reversed, adding an extra authentication step for the magneto-optical barcode and significantly enhancing the security of the safety label (Scheme 1). With this in mind, we seek to explore a new concept in security materials by creating magneto-optical barcodes accessed through magnetic circular dichroism (MCD) spectroscopy.[19–23]
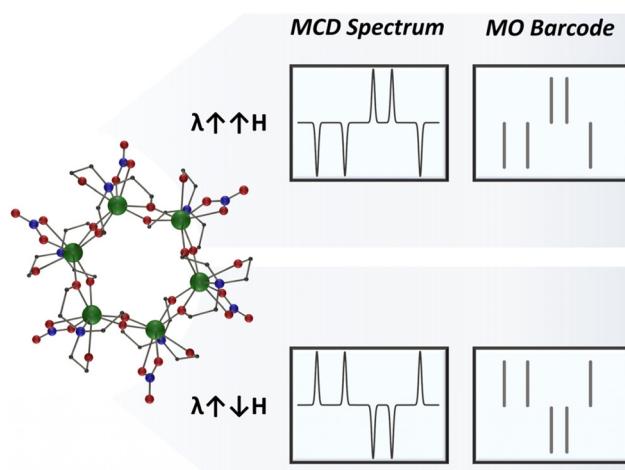
Scheme 1 (Left) Crystal structure of $[Er_6(teaH)_6(NO_3)_6]$, **{Er$_6$}** (colour code: green (Er); red (O), blue (N), black (C)) MCA (CCDC number: 1876163). (Right) representation of the dual-signalled magneto-optical barcode obtained *via* MCD spectroscopy.

In order to demonstrate for the first time the use of MCD as a readout platform for magneto-optical barcodes, we synthesized a hexanuclear molecular cluster-aggregate (MCA), $[Ln_6(teaH)_6(NO_3)_6]$, $\{Ln_6\}$, where $teaH^{2-}$ = doubly deprotonated triethanolamine as barcode material.[24,25] We opted to use MCAs because of the unique features offered by this class of compounds.[26–32] Their high nuclearity and molecular nature make MCAs a highly versatile optical material, mainly due to the possibility of controlling the metal composition at a single-cluster level, allowing us to target various optical signatures.

Our choice for the MCD technique relies on the intrinsic presence of MCD signals in all paramagnetic species, eliminating the need for chiral ligands to promote polarization or suitable ligands to sensitize the metal centre luminescence. Additionally, the spectral signature remains unique for the metal ion in a specific chemical environment.

With this objective in mind, we successfully synthesized three isostructural hexanuclear MCAs, namely $\{Ho_6\}$, $\{Er_6\}$, and $\{Ho_3Er_3\}$. The two homometallic MCAs were synthesized to investigate the individual fingerprint of each metal, while the heterometallic species allowed us to demonstrate the potential of enhancing barcode complexity by combining different metals within a single cluster unity. Powder X-ray diffractograms and FTIR confirm that we successfully obtained the targeted MCAs (Fig. S1 and S2†). Moreover, ICP-OES further validates the composition for the heterometallic MCA (calculated: 50% Ho, 50% Er; obtained 47.3% Ho, 52.7% Er).

As previously demonstrated, the $\{Ln_6\}$ MCA is soluble and stable in water,[24] as such we opted to investigate a water solution with a concentration of 0.1 mg mL^{-1} as a proof-of-concept system. The visible spectral range MCD spectra for $\{Ho_6\}$ and $\{Er_6\}$ obtained at 25 °C and with a magnetic field of 0.5, 1.0, and 1.5 T is depicted in Fig. 1. It is possible to observe the characteristic narrow f–f absorption bands arising from Ho^{III} $^5I_8$ and Er^{III} $^4I_{15/2}$ ground states. Another spectral feature is the magnetic field dependence of the observed bands, increasing upon the application of higher magnetic fields and the mirror image when applying an anti-parallel magnetic field in relation to the light beam ($\lambda\uparrow\downarrow H$). Both MCAs exhibit the presence of left (positive signal) and right (negative signal) circularly polarized transition bands. Furthermore, the spectral signature for $\{Ho_6\}$ and $\{Er_6\}$ contains negative and positive bands located at distinct positions, raising curiosity about what the spectral fingerprint for a heterometallic composition would resemble (see below). More importantly, each transition band was assigned according to the expected position summarized by Carnall (Fig. 2 and Table S1†).[33]

It should be noted that at this temperature range, MCD signals are temperature insensitive,[23] representing another advantage when compared with luminescent barcodes, which could require an extra calibration step due to the strong temperature dependence of luminescence signals close to room temperature.[34–38] Also, despite being usually weak at this temperature range, the use of MCAs with a large number of metal sites allowed us to observe strong signals at 25 °C and with a diluted aqueous solution (0.1 mg mL^{-1}).

The data presented in Fig. 1 inherently serves as a compelling proof-of-concept for MCD-based magneto-optical barcodes using MCAs. Nevertheless, our primary goal was to demonstrate that the amalgamation of MCD spectroscopy with MCAs enabled us to augment the level of complexity of these magneto-optical barcodes by combining the transitions of different lanthanide ions within a single MCA unit.

Variable-field MCD spectra for $\{Ho_3Er_3\}$ MCA are shown in Fig. S3,† revealing a tailored spectral signature containing signals from both ions. As for the homometallic MCAs, we observed the mirror image when inverting the magnetic field direction. The combination of bands arising from Ho^{III} and Er^{III}, occurring at slightly different energies and in some cases containing distinct polarization, resulted in a complex spectral signature. This complexity is manifested by the emergence of additional shoulders and splitting, making the spectral fingerprint more intricate and difficult to duplicate.
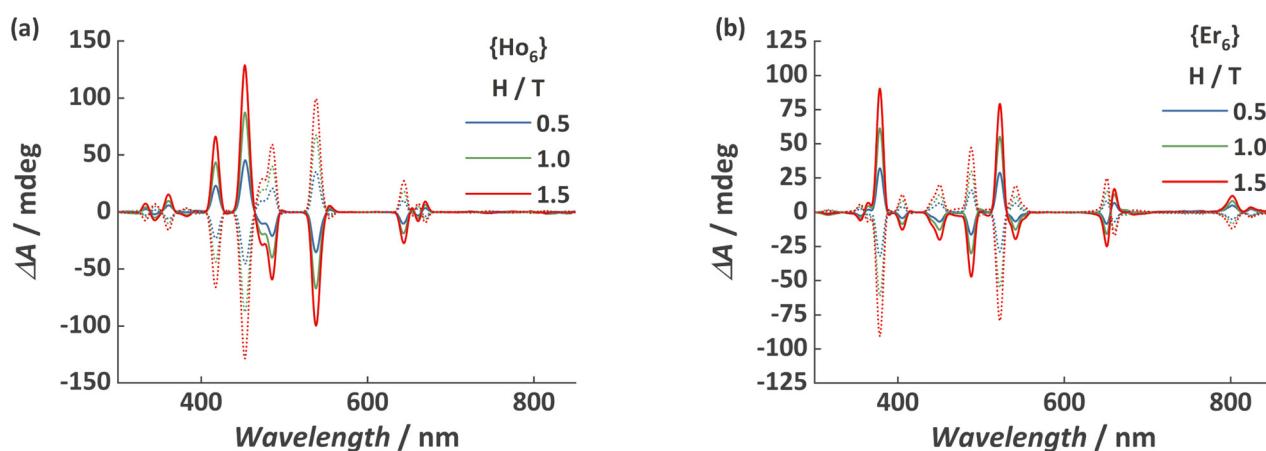
Fig. 1 MCD spectra for (a) $\{Ho_6\}$ and (b) $\{Er_6\}$ MCAs obtained at 25 °C and under various applied magnetic field. Dotted spectra refer to $H = -0.5$, -1.0, and -1.5 T magnetic field.
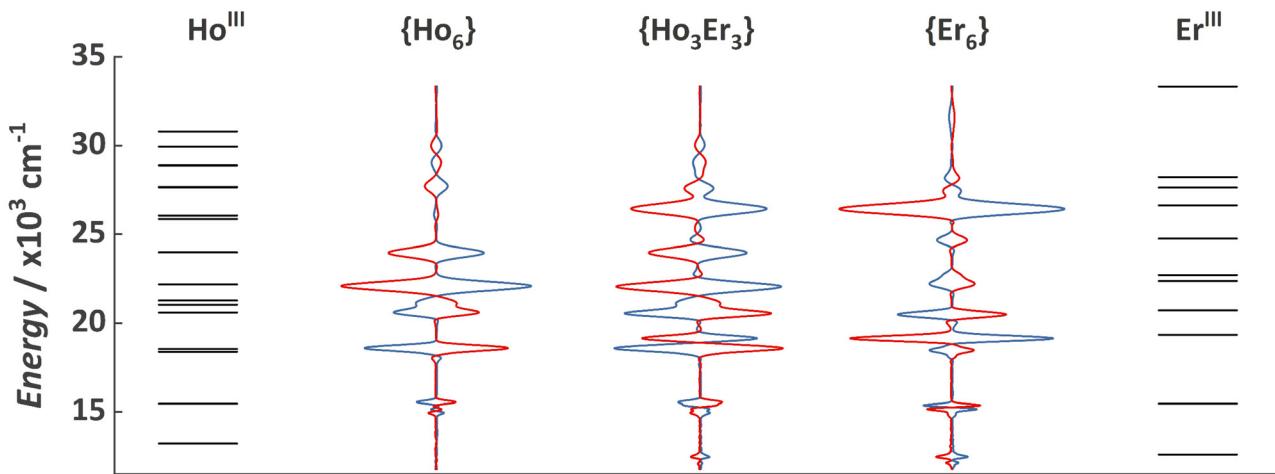
Fig. 2 Energy level diagram showing the excited states of Ho^{III} and Er^{III} and MCD spectra for **{Ho$_6$}**, **{Ho$_3$Er$_3$}**, and **{Er$_6$}** MCAs obtained under an applied magnetic field of 1.0 T (blue lines) and −1.0 T (red lines). Energy levels were obtained in Carnall book[33] and are summarized in Table S1.†

In an attempt to showcase the magneto-optical barcodes, we represented the dual-signalled signal in a manner similar to the widely used monochrome barcode (Fig. 3). This illustration highlights that these magneto-optical barcodes can exhibit much higher complexity compared to luminescent barcodes. Additionally, the mirror-image generated when inverting the direction of the applied magnetic field can be used as an extra authentication factor, offering the possibility of a three-factor authentication (3FA) magneto-optical barcode, specifically:

(1) Authentication of the left polarized transition bands (position and intensity of the positive signals);

(2) Authentication of the right polarized transition bands (position and intensity of the negative signals);

(3) Authentication of the mirror image upon field inversion.

The barcoding strategy represented in Fig. 3 is a simple yet elegant first proof-of-concept for magneto-optical barcodes. Future studies hold the potential to enhance the read-out strategy further. For example, it is possible to assign different weights depending on the band intensity, thus resulting in barcodes with different line thicknesses, akin to monochrome barcodes. Moreover, the use of variable magnetic fields might
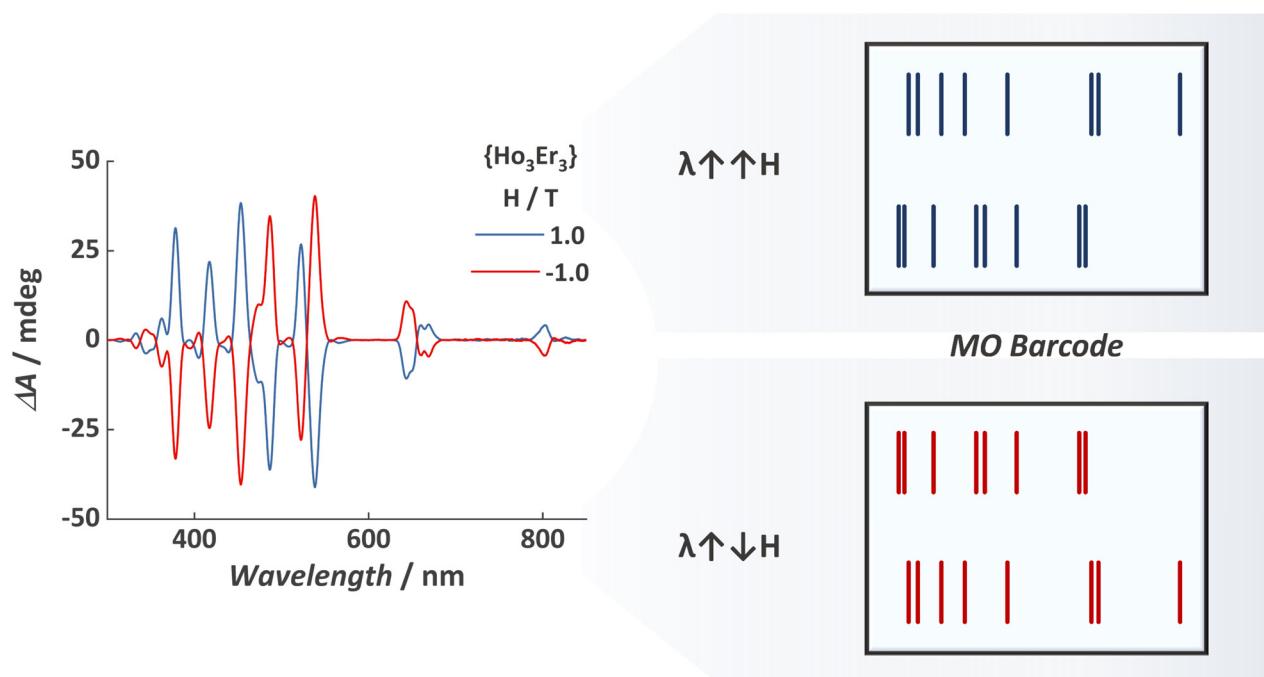

Fig. 3 (Left) MCD spectra for **{Ho$_3$Er$_3$}** and (right) representation of the magneto-optical barcode read-out. For an overlay of the read-out representation and MCD spectra, see Fig. S4 and S5.†

introduce a fourth authentication factor due to the strong magnetic field dependence of the MCD bands.

In our recent work related to magneto-optical thermometers based on MCD,[39] we discussed about some advantages, disadvantages, and challenges on using MCD spectroscopy for applications. The same challenges reported there are valid for the magneto-optical barcodes reported in this work, and we foreseen that further works on potential applications for MCD spectroscopy will help us to tackle these challenges.

Regarding potential candidates for magneto-optical barcodes, we anticipate that large nuclearity compounds such as MCAs, metal–organic frameworks, and nanoparticles could be used for obtaining heterometallic magneto optical barcodes with enhanced complexity. Nevertheless, we still believe in the superiority of MCAs when targeting synthetically reproducible compounds since metal–organic frameworks are known for the formation of composition "islands", and nanoparticles still suffer issues from the size distribution, which can lead to slightly different optical outputs when comparing different synthetic batches. In this regard, we foresee that MCAs with higher nuclearities could produce extremely more complex magneto-optical signatures by doping these large MCAs with more than two lanthanide ions.

Conclusions

In summary, we have successfully demonstrated a pioneering proof-of-concept for MCD-based magneto-optical barcodes. The dual-signalled spectral features observed *via* magnetic circular dichroism provide two authentication channels for the security label, with the left and right polarized transition bands displaying positive and negative signals, respectively. Additionally, the mirror-image obtained when inverting the magnetic field introduces a third authentication factor, significantly elevating the security level of these magneto-optical barcodes compared to other optical barcodes.

The findings presented in this study open new avenues for anti-counterfeiting materials and techniques, rendering the development of security labels much more challenging to counterfeit. These advancements have the potential to enhance security measures and protect governments, companies, and customers from the detrimental impacts of counterfeit goods and forged documents.

Conflicts of interest

There are no conflicts to declare.

Acknowledgements

References

1 J. Gooch, B. Daniel, V. Abbate and N. Frascione, *TrAC, Trends Anal. Chem.*, 2016, **83**, 49.

2 H. Omidian and Y. Omidi, *Drug Discovery Today*, 2022, **27**, 103335.

3 K. S. Ziavrou, S. Noguera and V. A. Boumba, *Forensic Sci. Int.*, 2022, **338**, 111382.

4 H. Zhang, D. Hua, C. Huang, S. K. Samal, R. Xiong, F. Sauvage, K. Braeckmans, K. Remaut and S. C. De Smedt, *Adv. Mater.*, 2020, **32**, 1905486.

5 W. Ren, G. Lin, C. Clarke, J. Zhou and D. Jin, *Adv. Mater.*, 2020, **32**, 1901430.

6 M. R. Carro-Temboury, R. Arppe, T. Vosch and T. J. Sørensen, *Sci. Adv.*, 2018, **4**, e1701384.

7 R. Arppe and T. J. Sørensen, *Nat. Rev. Chem.*, 2017, **1**, 0031.

8 Y. Xie, Y. Song, G. Sun, P. Hu, A. Bednarkiewicz and L. Sun, *Light: Sci. Appl.*, 2022, **11**, 150.

9 Y. Liu, K. Ai and L. Lu, *Nanoscale*, 2011, **3**, 4804.

10 J. Andres, R. D. Hersch, J.-E. Moser and A.-S. Chauvin, *Adv. Funct. Mater.*, 2014, **24**, 5021.

11 J. Yang, Y. Ping, H. Ma and L. Lei, *Nanoscale*, 2023, **15**, 4361.

12 R. Arppe-Tabbara, M. Tabbara and T. J. Sørensen, *ACS Appl. Mater. Interfaces*, 2019, **11**, 6475.

13 D. A. Gálico, A. A. Kitos, J. S. Ovens, F. A. Sigoli and M. Murugesu, *Angew. Chem., Int. Ed.*, 2021, **60**, 6130.

14 J.-C. G. Bünzli and S. V. Eliseeva, Basics of Lanthanide Photophysics, in *Springer Series on Fluorescence: Lanthanide Luminescence: Photophysical, Analytical and Biological Aspects*, ed. O. S. Wolfeis and M. Hof, Springer Verlag, Berlin, vol. 7, 2011.

15 J.-C. G. Bünzli, *Trends Chem.*, 2019, **1**, 751.

16 L. E. MacKenzie and R. Pal, *Nat. Rev. Chem.*, 2021, **5**, 109.

17 O. G. Willis, F. Zinna and L. Di Bari, *Angew. Chem., Int. Ed.*, 2023, **62**, e202302358.

18 F. Zinna and L. Di Bari, *Chirality*, 2015, **27**, 1.

19 Y. Kitagawa, S. Wada, K. Yanagisawa, T. Nakanishi, K. Fushimi and Y. Hasegawa, *ChemPhysChem*, 2016, **17**, 845.

20 C. Görller-Walrand and L. Fluyt, *Handb. Phys. Chem. Rare Earths*, 2010, **40**, 1.

21 R. W. Schwartz, H. G. Brittain, J. P. Riehl, W. Yeakel and F. S. Richardson, *Mol. Phys.*, 1977, **34**, 361.

22 A. Santria and N. Ishikawa, *Inorg. Chem.*, 2021, **60**, 14418.

23 N. J. Wolford, A. Radovic and M. L. Neidig, *Dalton Trans.*, 2021, **50**, 416.

24 D. A. Gálico, J. S. Ovens and M. Murugesu, *Nanoscale*, 2020, **12**, 11435.

25 S. K. Langley, B. Moubaraki, C. M. Forsyth, I. A. Gass and K. S. Murray, *Dalton Trans.*, 2010, **39**, 1705.

26 D. A. Gálico, C. M. S. Calado and M. Murugesu, *Chem. Sci.*, 2023, **14**, 5827.

27 Y.-L. Li, H.-L. Wang, Z.-H. Zhu, F.-P. Liang and H.-H. Zou, *Coord. Chem. Rev.*, 2023, **493**, 215322.

28 X.-Y. Zheng, J. Xie, X.-J. Kong, L.-S. Long and L.-S. Zheng, *Coord. Chem. Rev.*, 2019, **378**, 222.

29 A. T. Wagner and P. W. Roesky, *Eur. J. Inorg. Chem.*, 2016, **2016**, 782.

30 D. A. Gálico and M. Murugesu, *Angew. Chem., Int. Ed.*, 2022, **61**, e202204839.

31 K. Sheng, W.-D. Si, R. Wang, W.-Z. Wang, J. Dou, Z.-Y. Gao, L.-K. Wang, C.-H. Tung and D. Sun, *Chem. Mater.*, 2022, **34**, 4186.

32 R. C. Knighton, L. K. Soro, L. Francés-Soriano, A. Rodríguez-Rodríguez, G. Pilet, M. Lenertz, C. Platas-Iglesias, N. Hildebrandt and L. J. Charbonniere, *Angew. Chem., Int. Ed.*, 2022, **61**, e202113114.

33 A. W. T. Carnall, H. Crosswhite and H. M. Crosswhite, *Energy level structure and transition probabilities in the spectra of the trivalent lanthanides in LaF₃*, Argonne Nat. Lab. 78-XX-95 Rep., 1977.

34 T. P. van Swieten, J. M. Steenhoff, A. Vlasblom, R. de Berg, S. P. Mattern, F. T. Rabouw, M. Suta and A. Meijerink, *Light: Sci. Appl.*, 2022, **11**, 343.

35 C. D. S. Brites, P. P. Lima, N. J. O. Silva, A. Millán, V. S. Amaral, F. Palacio and L. D. Carlos, *Nanoscale*, 2012, **4**, 4799.

36 C. D. S. Brites, S. Balabhadra and L. D. Carlos, *Adv. Opt. Mater.*, 2019, **7**, 1801239.

37 A. M. Kackzmarek, Y. Maegawa, A. Abalymov, A. G. Skirtach, S. Inagaki and P. Van Der Voort, *ACS Appl. Mater. Interfaces*, 2020, **12**, 13540.

38 D. A. Gálico and M. Murugesu, *ACS Appl. Mater. Interfaces*, 2021, **13**, 47052.

39 D. A. Gálico and M. Murugesu, *Angew. Chem., Int. Ed.*, 2023, **62**, e202309152.